A STUDY OF TRANSIENT RADIATION EFFECTS ON THE RESPONSE OF STANDARD AND RADIATION-HARDENED INTEGRATED-CIRCUIT OPERATIONAL AMPLIFIERS IN AN ELECTRON BEAM

Patric Stam Enright

United States
Naval Postgraduate School

THESIS

A STUDY OF TRANSIENT RADIATION EFFECTS
ON THE RESPONSE OF STANDARD AND RADIATION-HARDENED
INTEGRATED-CIRCUIT OPERATIONAL AMPLIFIERS
IN AN ELECTRON BEAM

by

Patric Stam Enright

December 1969

A Study of Transient Radiation Effects on the Response of Standard and Radiation-Hardened Integrated-Circuit Operational Amplifiers in an Electron Beam

by

Patric Stam Enright
Captain, United States Marine Corps
B.S., United States Naval Academy, 1963

Submitted in partial fulfillment of the
requirements for the degree of

MASTER OF SCIENCE IN ELECTRICAL ENGINEERING

from the

NAVAL POSTGRADUATE SCHOOL
December 1969

ABSTRACT

This study investigates the effects of 1-μsec pulses of 80 - 90 Mev electrons on the standard μA709 operational amplifier and its radiation-hardened version, the μA744. The transient responses from the electron beam and from electronic pulses were investigated and compared for each amplifier. Also investigated were the responses of dielectrically isolated NPN and PNP transistors contained in the μA744, which were further compared with responses obtained from discrete NPN and PNP transistors.

The overall transient radiation responses of the μA709 and μA744 amplifiers, with several exceptions, were not very different. The same can be said for a comparison of the responses from the μA744 and discrete NPN and PNP transistors. Based on this study the μA744 is not superior to the μA709 by virtue of its radiation hardening. It should be noted, however, that the μA709 is driven into oscillation by the electron beam while the μA744 is not.

TABLE OF CONTENTS

LIST OF TABLES

LIST OF ILLUSTRATIONS

ACKNOWLEDGEMENTS

The author wishes to extend particular appreciation to the following individuals for their time and assistance in the preparation of this study:

Professor John N. Dyer and Professor Shu-gar Chan, my thesis advisors.

Professor Franz Bumiller and Professor Fred Buskirk for the use of the NPS linear accelerator, and to Mr. Don Snyder, technician.

Mr. Kenneth Stafford of the Linear Integrated Circuits Section of Fairchild Semiconductor's Research and Development Laboratory for providing circuits and technical data.

My wife, Jane, for her patience, encouragement, and for typing my first draft.

I. INTRODUCTION

In this era of rapid development in nuclear weaponry and space exploration, particular attention must be paid by the advancing field of integrated circuitry to radiation environments, their effects on integrated-circuit operation, and the development of more efficient techniques of radiation hardening.

There are two basic kinds of radiation environments. The first is transient radiation which appears as high-intensity, short-duration pulses such as produced by a nuclear weapon burst. The second is the steady-state environment which is encountered in nuclear reactors and in outer space from sources such as the Van Allen belts.

This study concerned itself solely with an investigation of the transient effects of the transient radiation environment from a linear electron accelerator on the responses of Fairchild μA709 and μA744 operational amplifiers. The radiation considered was that obtained from 80-90 Mev electrons.

It should be noted that the investigation and comparison of permanent damage to the μA709 and μA744 from large accumulated doses of the same radiation were investigated by LT D. F. Lesemann in his thesis entitled Comparison Between Radiation-Hardened and Standard Integrated-Circuit Amplifiers in an Electron Beam. The present study, combined with that done by Lesemann, constitutes the total investigation on these circuits conducted at the Naval Postgraduate School to date.

II. DISCUSSION AND COMPARISON OF THE μA709 AND μA744 AMPLIFIERS AND THEIR COMPONENT PARTS

The μA709 high-performance operational amplifier is a commercially available, general-purpose, high-gain device. It is constructed in monolithic form by the Fairchild Planar epitaxial method on a 55-mil-square silicon chip. Some of its applications include use in the generation of special linear and nonlinear transfer functions, high-impedance analog computers, low-level instrumentation, and DC servo systems. [1]

As is common to most integrated operational amplifiers, the μA709 consists of three basic stages.

The input stage employs a Darlington input amplifier designed in such a way as to minimize or eliminate difficulties encountered with this type of input amplifier.

The intermediate or second stage, with its inherent isolation from variations in supply voltages, provides conversion from differential to single-ended connection, as well as temperature stability. Prevention of second-stage loading from the output stage by use of an emitter follower, and prevention of loading of the input stage from the second stage by use of a modified Darlington configuration are other important built-in features.

The output stage employs a level-shifting technique from the second stage, which can operate with current gains less than 0.2. This stage is a complementary Class-B amplifier which is designed to prevent latch-up or runaway under overload conditions. [2]

This particular operational amplifier possesses the following features: low offset, high input impedance, high gain, large output swing under load, low power consumption, and a large input common-mode range.

A complete schematic diagram of the μA709 is shown in Figure 1.

In order to gain a more complete understanding of radiation response not only were the responses of the whole amplifiers studied, but also those of the individual, active amplifier components as well. To enable this testing of individual amplifier components Fairchild Semiconductor fabricated, in addition to complete amplifiers, amplifier circuits that contained lead bonding only to the individual transistors. These circuits with only transistor lead bondings were called kit parts. The μA709 kit part chosen for testing was designated KP-1 and its lead bonding and component identification are shown in Table 1.

In military application of integrated circuits attention must be given to radiation effects, and subsequently radiation-hardened circuits. There are two types of radiation that have significant effects on integrated circuits. [3] The first is ionizing radiation which creates photocurrents in semiconductor junctions; these currents are dependent on dose rate, junction area, and bias voltage. At lower dose rates the circuits are perturbed only electrically whereas at much higher rates permanent circuit damage may occur. Over a long period of time effects are further dependent on total accumulated dose. The second type of radiation is that caused by neutrons, which cause primarily permanent damage to integrated circuits by bulk displacements. In the course of this study only ionizing radiation effects caused by 80-90 Mev electrons were investigated.

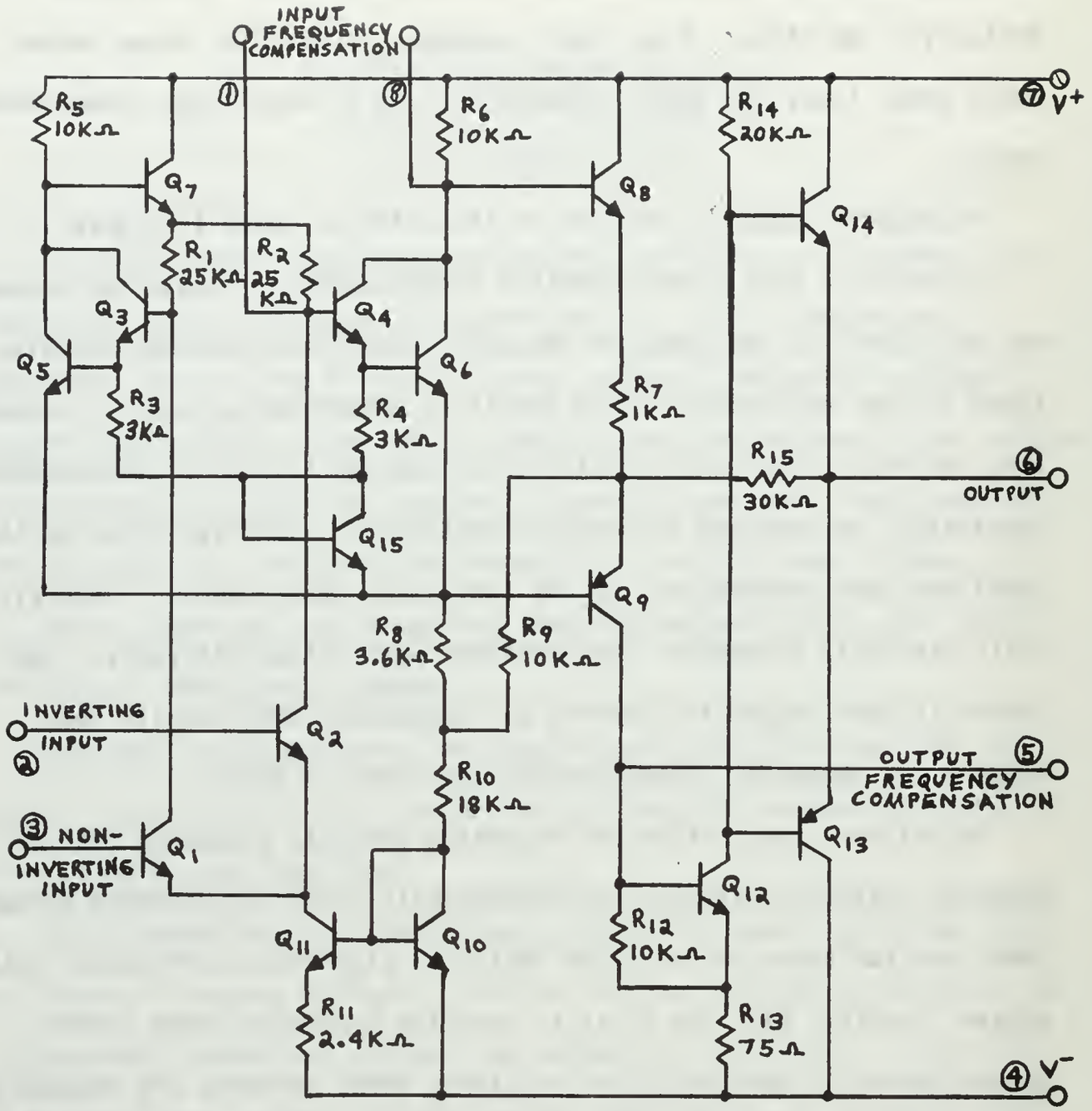

Figure 1. Schematic of the μA709 Operational Amplifier

COMPONENT	LEAD NUMBERS			
	COLLECTOR	BASE	EMITTER	SUBSTRATE
SMALL GEOM. NPN	1	3	2	4
SMALL GEOM. NPN	7	6	5	4

Table 1. KP-1 Components and Lead Bonding

The μA744 is essentially the same operational amplifier as the μA709 except for the radiation-hardening techniques used in it fabrication.

In order to achieve this hardening certain fabrication techniques and materials were utilized. Among the more important of these were: thin film resistors instead of diffused resistors to limit the photocurrent flow between power supplies during irradiation; dielectric isolation vice PN-junction isolation to prevent radiation-generated photocurrents from flowing across isolating junctions, thus minimizing excessive substrate currents and four-layer latch-up; and, gettering and silicon-nitride passivation techniques to insure NPN and PNP transistors having high h_{FE} and long-term stability. Another technique employed to minimize the effects of photocurrents was the addition of photocurrent-compensation diodes. [4] The location of these diodes can be found in Figure 2, which is a complete schematic of the μA744. [5]

The radiation-hardening technique called dielectric isolation, which calls for the construction of individual transistors and other circuit elements encapsulated in silicon dioxide, is explained in detail with accompanying diagrams in Lesemann's thesis. [6]

As was done in the case of the μA709, Fairchild Semiconductor fabricated and packaged a series of kit parts from the μA744. Only one of these kit parts, designated KP-5, was used as a test subject for this study. The KP-5 lead bonding and component identification are contained in Table 2.

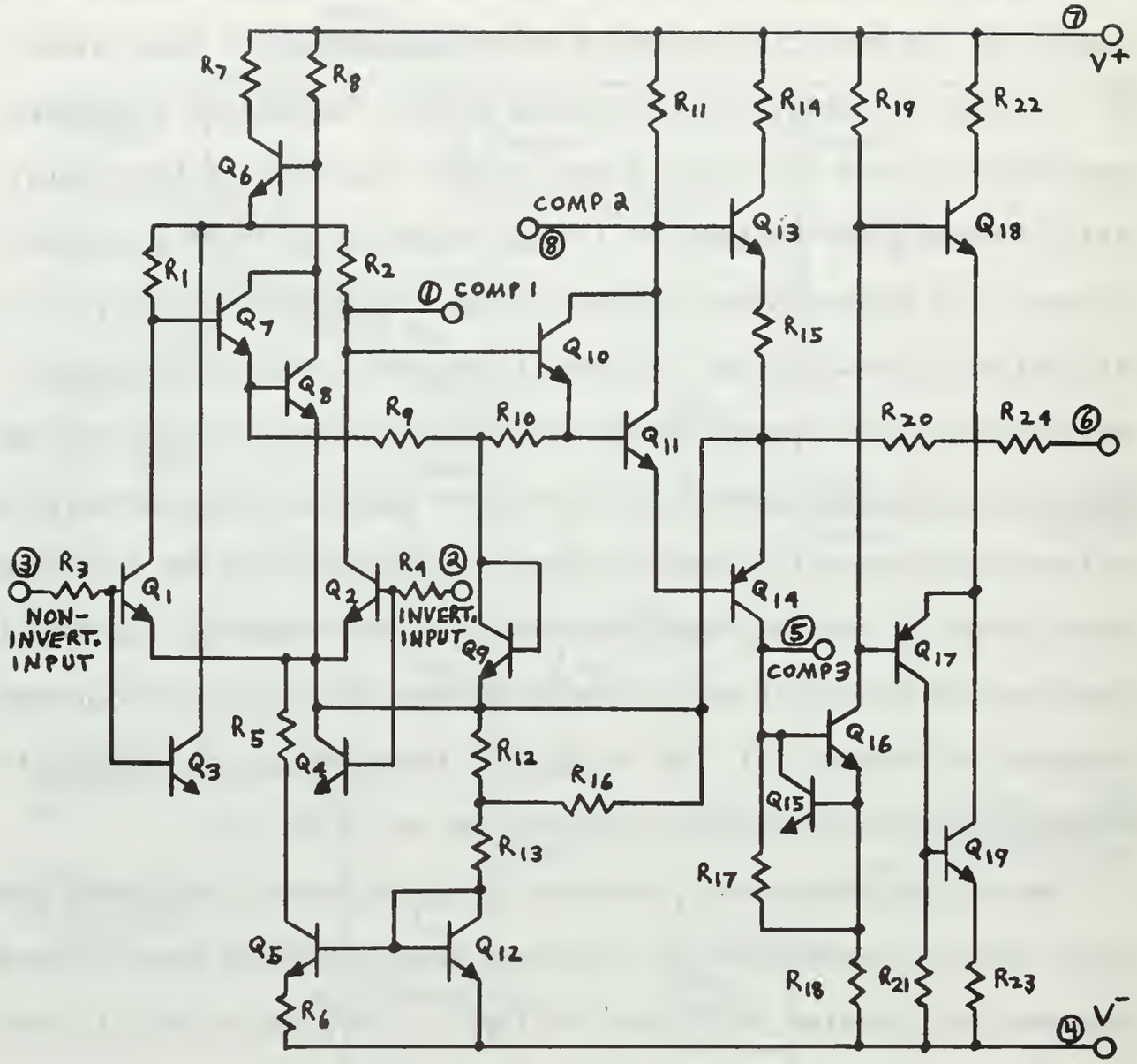

Figure 2. Schematic of the μA744 Operational Amplifier

COMPONENT	LEAD NUMBERS			
	COLLECTOR	BASE	EMITTER	SUBSTRATE
SMALL GEOM. NPN (Q_{11})	7	6	5	NONE
SMALL GEOM. PNP (Q_{14})	3	4	2	NONE

Table 2. KP-5 Components and Lead Bonding

III. TESTS PERFORMED ON THE μA709

The radiation tests run on the μA709 amplifier were those which provided data on changes in pulse width, response amplitude (amplifier gain), response recovery time, and spurious response occurrence. These tests consisted of the following inputs and parameter variations: 1-microsecond electron-beam pulses, 10-microsecond electronic pulses, varied beam intensities, varied amplifier-biasing voltages and variations in the timing of input-pulse perturbations. Polaroid photographs provided the bulk of observed response data.

A. μA709 TEST CIRCUITRY, EQUIPMENT, AND PROCEDURES

The circuit used for testing μA709 operational amplifiers was recommended by Fairchild Semiconductor. [7] The schematic of this test circuit with the appropriate frequency compensation, impedance matching, and attenuation elements added is illustrated in Figure 3.

The μA709 and its test circuitry were placed in an aluminum box (Figure 4), which in turn was positioned on a remotely controlled platform. The platform could be moved horizontally and vertically, thus enabling the μA709 to be positioned in the center of the electron beam. The positioning of the circuit was monitored by closed-circuit television. In order to tell when the circuit was correctly positioned in the electron beam, each circuit was painted with phosphor paint, which would glow when excited by the electrons. The movable platform was controlled from the LINAC control station.

The ±15-v supply voltages were supplied from two Hewlett-Packard 721A DC power supplies, and the electronic input pulse was provided by a

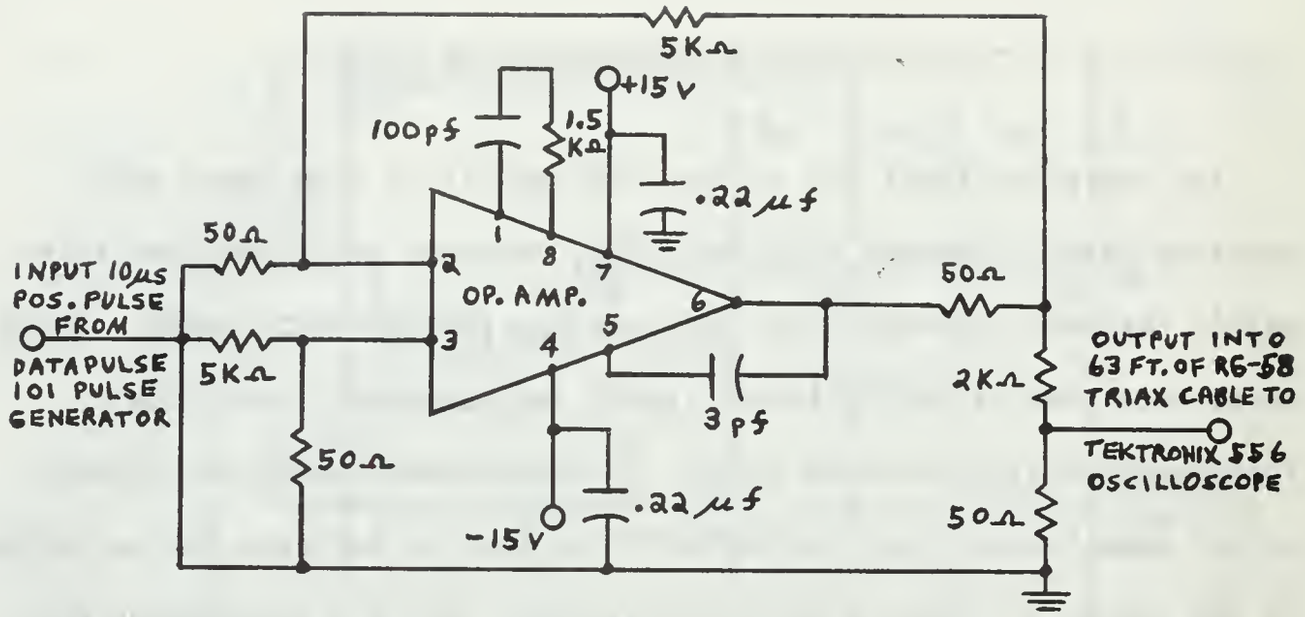

Figure 3. Schematic of μA709 and μA744 Test Circuit

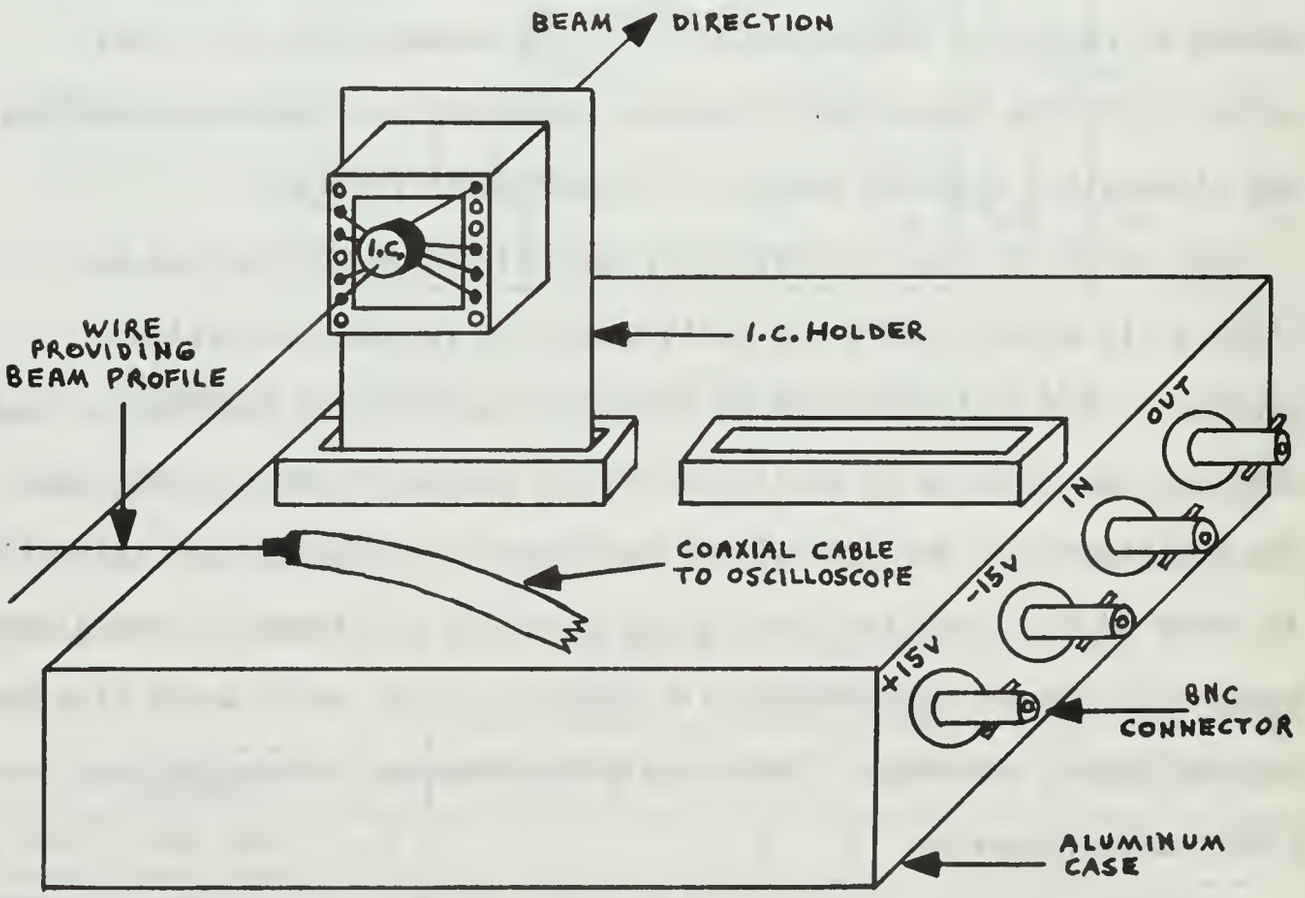

Figure 4. Diagram of μA709 and μA744 Test Box

Datapulse 101 pulse generator. The input pulse and output response were monitored on a Tektronix 556 oscilloscope. Monitoring of the dosage was accomplished by a Faraday cup. In all cases single 1-microsecond beam pulses were employed to perturb the operational amplifiers. This was done so that the inputs to the amplifier would be restricted to electronic and electron-beam pulses, and to insure that the radiation environment was purely transient, thus avoiding large accumulated dosages of high-intensity radiation which would cause permanent circuit damage.

The first tests conducted on the μA709 gave relative responses to varying beam strength and supply voltages on the amplifier transient response. In these tests, the beam strength was varied by moving the circuit in and out of the beam path. This method did not provide a quantitative measure of the beam strength or dosage, but only provided a sample of the relative radiation effects with varying supply voltages and a constant electronic-pulse input. A thin conducting wire, attached to a coaxial cable, was positioned in the beam path so as to provide a time profile of the electron beam (Figure 4). The coaxial cable was in turn connected to the Tektronix 556 oscilloscope in order to provide time-profile displays of the beam pulse which perturbed the circuit. The beam and electronic pulses did not perturb the circuit simultaneously.

In the second set of tests quantitative dose measurements were obtained. These measurements were taken directly from a vibrating-reed electrometer which was attached to the Faraday cup. The dose values were read in millivolts which were in turn converted to rads. This conversion is discussed at length in Appendix A. These tests were also conducted with varying supply voltages and a constant electronic-pulse input.

The third set of tests was conducted in the same manner as the first two, except that the data were divided into two groups. One group was taken under the following conditions. The circuit was first perturbed by the beam pulse and then, approximately 20-microseconds later, it amplified the electronic pulse. This was done so as to see how quickly the circuit recovered from the effects of the beam pulse. The other data group was taken when the beam pulse perturbed the circuit at the same time the circuit was amplifying the electronic pulse. The entire series of tests was performed on circuits which had had no previous exposure to radiation. After each set of data was taken, however, these same circuits were exposed to the following progression of radiation doses: 8.6×10^6, 1.7×10^7, 3.4×10^7, 6.8×10^7, and 5.1×10^8 rads.

B. DISCUSSION OF RESULTS (μA709)

In the first test, the photographs (Figure 5) show the responses to increased beam strength and varying supply voltages. The top row of pictures in Figure 5 was taken with both supply voltages at 15 volts, and the bottom row with both supplies at 10 volts. The lower trace in each picture is the time profile of the beam pulse that perturbed the circuit. The top trace shows the amplifier response to the beam pulse on the left and to the electronic pulse on the right. Note that the horizontal sweep rates are not the same for the upper and lower traces. Since it was stated that the beam and electronic pulses were not perturbing the circuit simultaneously, the responses to these pulses are also not occurring simultaneously. In fact, each of the pictures in Figure 5 shows the circuit as having recovered from the beam-pulse perturbation before responding to the electronic pulse.

As the beam intensity increased the response-pulse amplitude increased up to the amplifying limit of the circuit, and the circuit recovery time

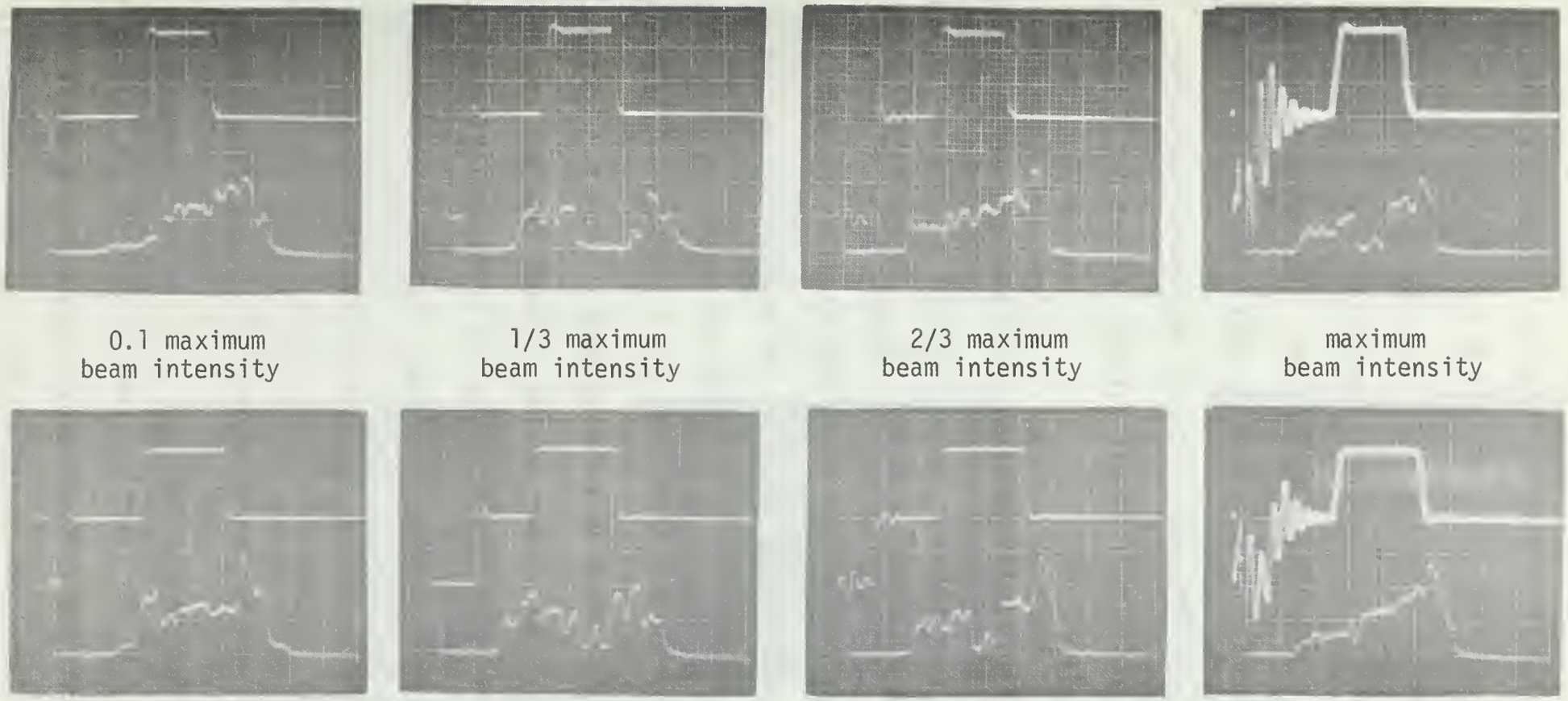

0.1 maximum beam intensity | 1/3 maximum beam intensity | 2/3 maximum beam intensity | maximum beam intensity

Upper Trace—Sweep: 5μsec/cm, Vert.: 0.1v/cm Lower Trace—Sweep: 0.2μsec/cm, Vert.: .05v/cm
Electronic Input Pulse—Amplitude: 10v, Width: 10μsec Top Row—V_S=±15v Bottom Row—V_S=±10v
(Traces are plotted in volts vs. time and the large scale squares measure 1 cm on a side.)

Figure 5. μA709: First Test Responses

increased. The increase in recovery time occurred a little more rapidly when the supply voltages were reduced to 10 volts. Up to the point where the circuit was receiving approximately 2/3 of the maximum beam intensity the beam-pulse response showed no evidence of oscillation or spurious response. However, as the circuit was exposed to increased beam intensity, it broke into strong oscillation. The oscillation became so strong under maximum beam intensity that the pulse shape of the response was almost obliterated. Although the overall amplifier gain was lowered by a reduction in supply voltages it was not affected by increased beam intensity.

In the second set of tests the beam and electronic pulses again did not perturb the circuit simultaneously. The purpose of these tests was to observe what happened to the amplifier's response to the beam and electronic pulses when supply voltages were decreased and the beam intensity remained the same for each pulse. The supply-voltage variations were divided into three groups. In all groups the progression of reduction was as follows: 15, 10, 7.5, 5.0, 2.5, and 1.0 volts. In the first group both the positive and negative voltages were reduced simultaneously, and Figure 6 gives a pictorial history of the response changes. As the supply voltages are decreased the gain of the electronic-pulse response is reduced while the recovery time is increased. At the same time the gain, as well as the recovery time of the beam-pulse response, is decreased. At the lowest point of supply voltage (1.0v) there remains a small beam-pulse response with a short recovery time but there is no electronic-pulse response.

The second group of data was taken in order to observe the effects of reduced gain, and increased and reduced recovery times, as a result of reduced supply voltage. Here, the positive supply was held constant at

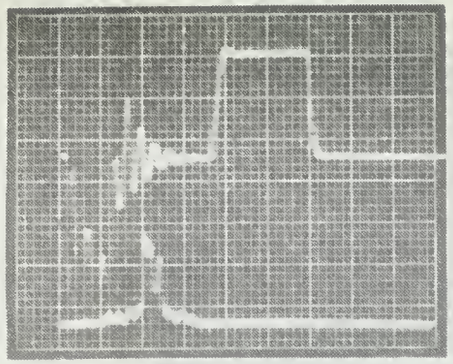

a. $V_s = \pm 15v$
5.4×10^3 rads

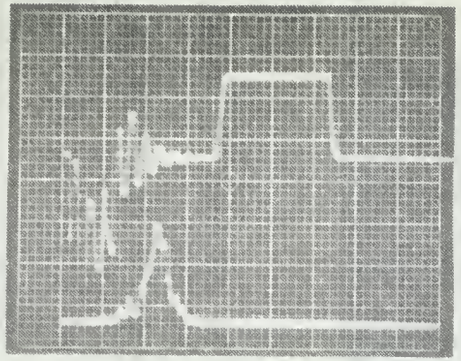

b. $V_s = \pm 10v$
6.8×10^3 rads

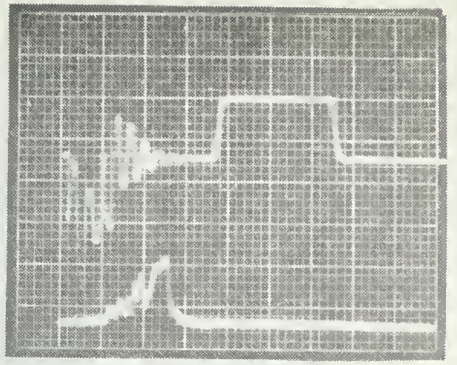

c. $V_s = \pm 7.5v$
6.3×10^3 rads

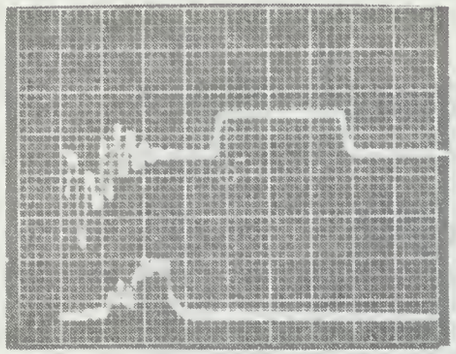

d. $V_s = \pm 5.0v$
6.8×10^3 rads

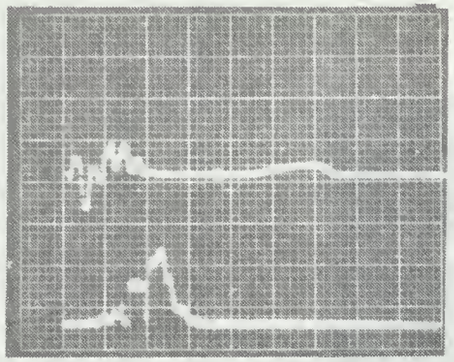

e. $V_s = \pm 2.5v$
6.3×10^3 rads

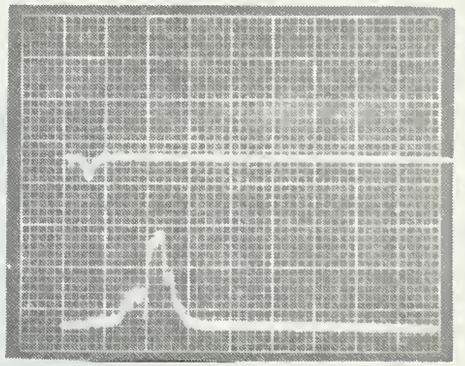

f. $V_s = \pm 1.0v$
6.8×10^3 rads

Upper Trace—Sweep: 5μsec/cm, Vert.: 0.1v/cm Lower Trace—Sweep: 0.5μsec/cm, Vert.: 0.01v/cm
Electronic Input Pulse—Amplitude: 10v, Width: 10μsec
(Traces are plotted in volts vs. time and the large scale squares measure 1cm on a side.)

Figure 6. μA709: Second Test Responses (Group 1)

15 volts while the negative supply was reduced. The maximum and minimum negative-supply responses are shown on the top row of Figure 7. By reducing only the negative supply there was no significant change observed in either of the circuit responses, except for a slight reduction in the oscillations produced in the beam-pulse response and this response's recovery time.

The third group of data was taken while the negative supply was held at a constant 15 volts and the positive supply was reduced. The bottom row of pictures in Figure 7 shows the maximum and minimum negative-voltage responses. The electronic-pulse response shows a total drop in amplitude while the beam-pulse response shows some amplitude drop, a marked reduction in response recovery time, and a decrease in the severity of oscillations.

The electronic-pulse response is affected only by changes in negative, or positive and negative supply voltages. The beam-pulse response is affected in a similar manner but the effect is not as great as it is in the electronic-pulse response. Also, the circuit continues to oscillate in the presence of the beam pulse with the oscillations being somewhat reduced by a drop in negative, or both positive and negative, supply voltages.

The causes of the circuit oscillations were not evident during testing, but it was felt that the supply voltage-decoupling capacitances (Figure 3) were too low. In the first two tests this capacitance was set as 0.01-microfarad and strong oscillations were observed. In the third test a value of 0.22-microfarads was used and the level of oscillation was reduced. Higher values of capacitance were used but they did not significantly reduce the level of oscillation and the latter value was

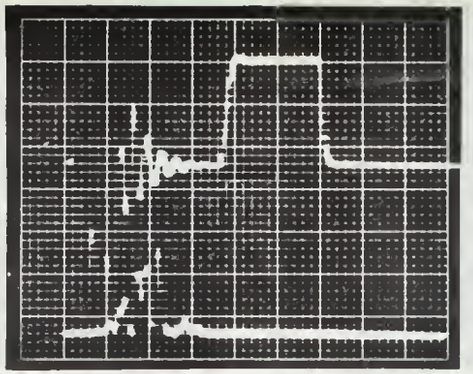

a. $V_s = \pm 15v$
4.6×10^3 rads

Group 2

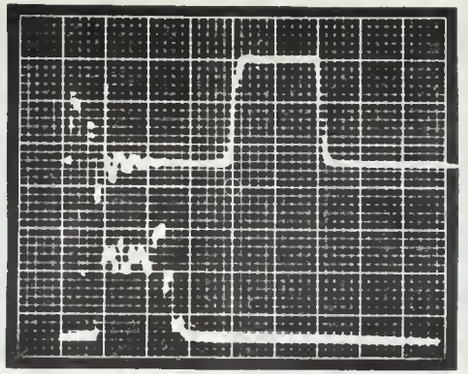

b. $V_s = +15v, -1v$
1.2×10^4 rads

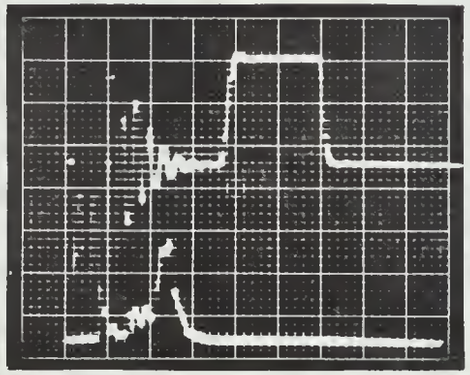

c. $V_s = \pm 15v$
7.4×10^3 rads

Group 3

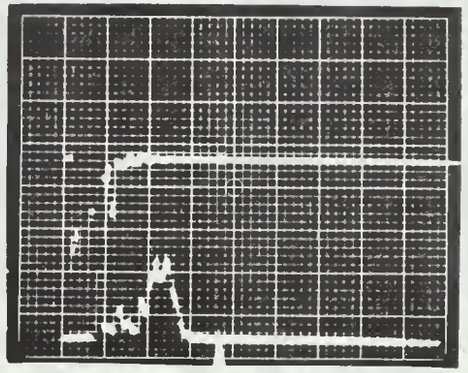

d. $V_s = +1v, -15v$
7.4×10^3 rads

(Scaling, electronic-input pulse, trace-plot, and large-scale square parameters are the same as in Figure 6.)

Figure 7. µA709: Second Test Responses (Groups 2 & 3)

used for all remaining tests. It is significant that only the beam pulse and not the electronic pulse caused oscillations.

The third test was set up to investigate the circuit response to separate and simultaneous pulse perturbations while reducing the beam intensity and holding the supply voltages constant at 15 volts. As was mentioned previously, the circuit was also subjected to varying amounts of increased dosage between data groupings to observe the effect of accumulated dose on the circuit response. Figures 8, 9, and 10 show the circuit responses after increased amounts of accumulated dose. All responses in Figures 8, 9, and 10 show a reduction in beam-response oscillation as a result of increased decoupling capacitance. The top rows of Figures 8 and 9 are for non-simultaneous circuit perturbance and the bottom rows are for simultaneous perturbance. Figure 10 shows only non-simultaneous perturbance responses. The top row of pictures in Figure 8 shows the further reduction of beam-response circuit oscillation with decreased beam intensity and no effect on the electronic-pulse response. As the beam intensity decreases the beam response takes the shape of the electronic response with a recovery time approaching that of the 1.0-microsecond input pulse width. The bottom row of Figure 8 illustrates what happens to the electronic-pulse response when the circuit is perturbed by the beam pulse during the time it is amplifying the electronic pulse. In this case the beam pulse causes a swamping-out of the electronic-pulse response. All other effects on the responses remain the same as those discussed in the top-row pictures.

Figure 9 is essentially the same response history as Figure 8 except that at this point the circuit has been exposed to a total dose of 1.3×10^8 rads. The added dose has no effect on the overall gain of the amplifier. The electronic-pulse response shows almost no change except for the

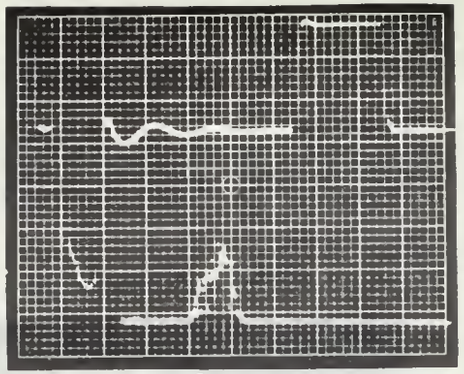

8.0×10^3 rads

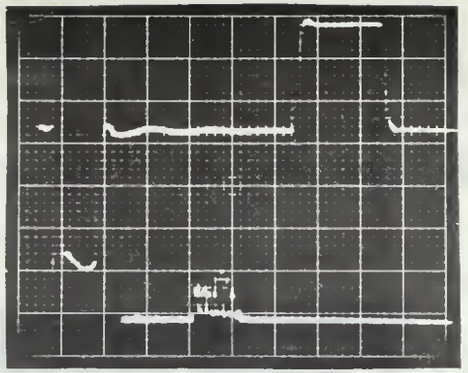

3.4×10^3 rads

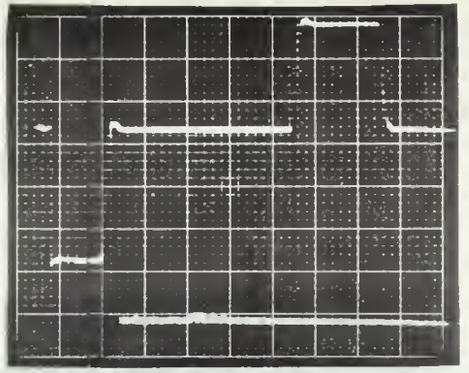

4.3×10^2 rads

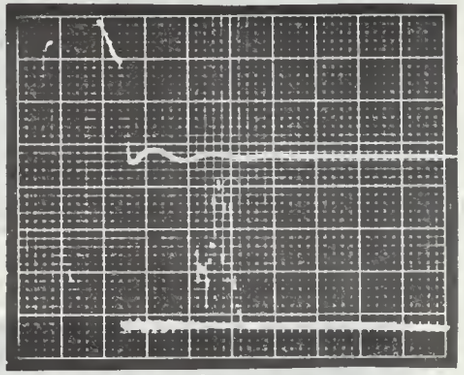

1.3×10^4 rads

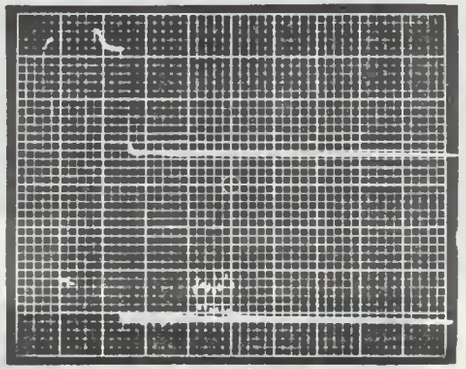

4.0×10^3 rads

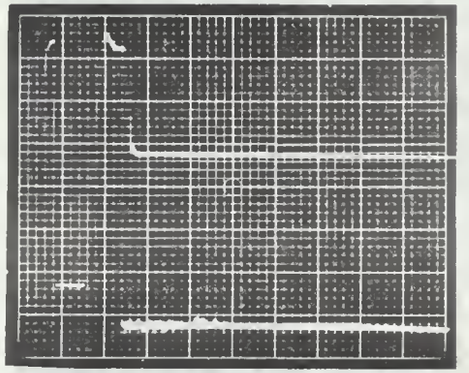

8.6×10^2 rads

Upper Trace—Sweep: 5μsec/cm, Vert.: 0.1v/cm Lower Trace—Sweep: 1μsec/cm, Vert.: 0.01v/cm
Electronic Input Pulse—Amplitude: 10v, Width: 10μsec
(Traces are plotted in volts vs. time and the large scale squares measure 1cm on a side.)

Figure 8. μA709: Third Test (no Accumulated Dose)

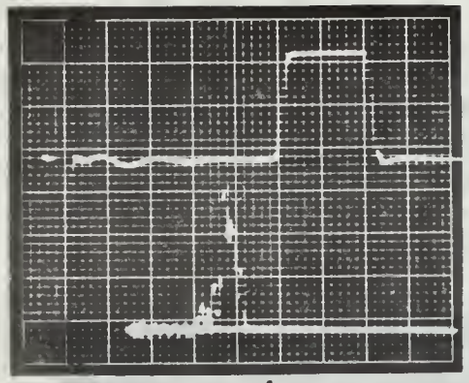

1.0×10^4 rads

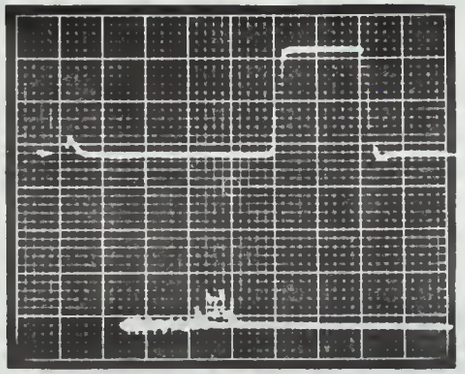

2.9×10^3 rads

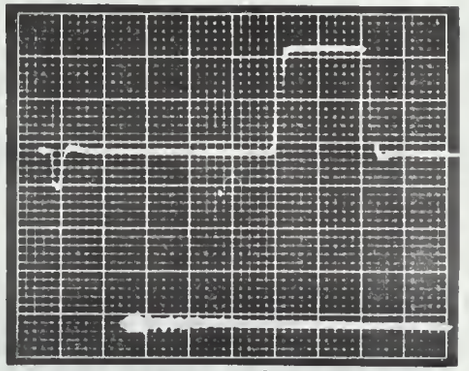

5.7×10^2 rads

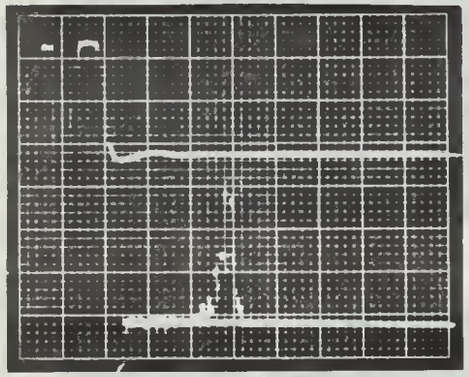

8.6×10^3 rads

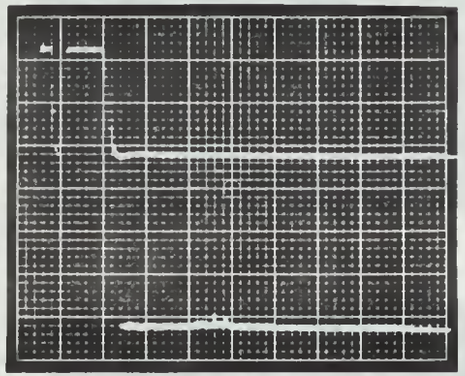

8.6×10^2 rads

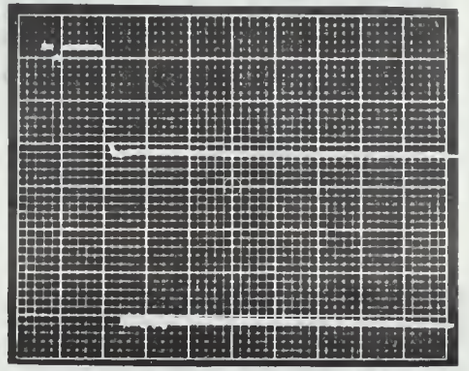

2.9×10^2 rads

(Scaling, electronic-input pulse, trace-plot, and large scale square parameters are the same as in Figure 8.)

Figure 9. μA709: Third Test (1.3×10^8 rads added dose)

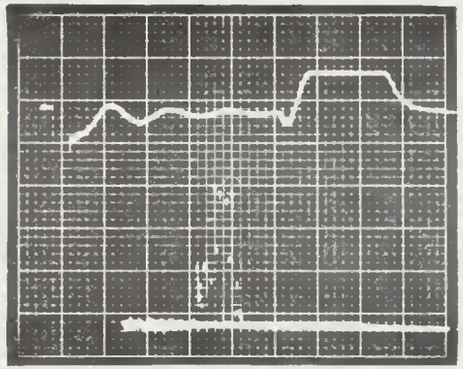

1.3×10^4 rads

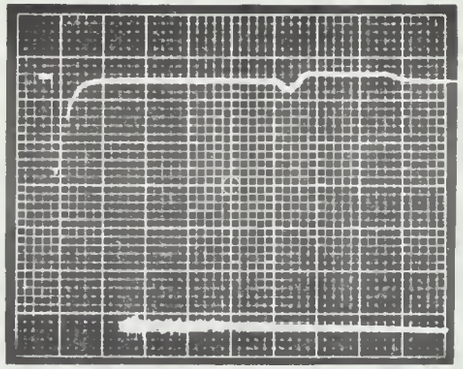

1.1×10^3 rads

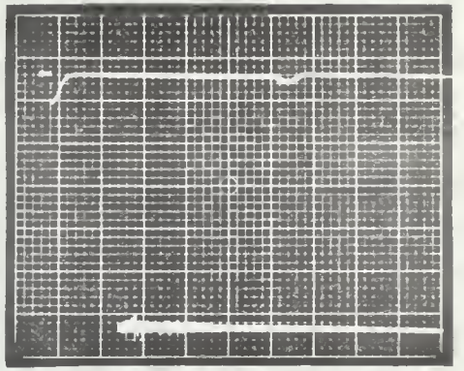

1.1×10^2 rads

(Scaling, electronic input pulse, trace-plot, and large scale square parameters are the same as in Figure 8.)

Figure 10. μA709: Third Test (6.4×10^8 rads added dose)

absence of the overshoot in the rise portion of the response. The most significant change is the reduction of the beam-pulse response width. It has now dropped from 1.0-μsec to 0.4-μsec. This effect appears to be caused by the higher dose level accumulated by the amplifier. The swamping-out of the electronic pulse still occurs as it did in Figure 8. A comparison of Figures 8 and 9 shows that the μA709 amplifier response to an electronic pulse is affected to a lesser extent after it has accumulated some measure of dosage than before accumulation of dose. This holds true when both "accumulated" and "non-accumulated" circuits are perturbed by electron-beam pulses of nearly the same intensity.

This apparent "hardening" of the μA709 is dependent upon the amount of total dosage accumulated. Figure 10 shows what happens to the circuit responses when too much dosage (6.4×10^8 rads) is accumulated by the amplifier. Not only is the overall amplifier gain reduced but now the magnitude of the electronic-pulse response seems to depend directly upon the magnitude of the beam-pulse response. At this point the μA709 is showing marked effects from too much radiation.

IV. TESTS ON μA709 KIT PART KP-1

Since the collector of KP-1 was tied to the integrated-circuit's substrate, it presented a most difficult obstacle in constructing a test circuit that would give a desired radiation and electronic-pulse response. After many repeated attempts at designing such a circuit the result was still no response. Thus no further attempt was made to investigate the individual μA709 amplifier transistors and compare these results to those of similar discrete off-the-shelf transistors.

V. TESTS PERFORMED ON THE μA744

A. μA744 TEST CIRCUITRY, EQUIPMENT, AND PROCEDURES

Since the μA744 possesses essentially the same operating characteristics as the μA709 amplifier, the same test circuitry and test box were used for this amplifier. Diagrams of the test circuitry and test box can be seen in Figures 3 and 4. Also, all monitoring, pulse, and voltage-supply equipment is the same as that used for the μA709.

The first set of tests is the same as that run on the μA709. These tests show a relative radiation response with varying beam intensity. The variation in beam intensity is obtained by physically moving the circuit in and out of the beam path. The Faraday cup was not in position and no quantitative dose measurements were taken.

The second set of tests was similar to that with the μA709 in that it shows the change in response with varying supply voltages and essentially constant beam intensity.

The third set of tests was again conducted in the same manner as on the μA709. In these tests the increased decoupling capacitance (0.22-μF) was used in the test circuitry to eliminate any oscillations that might appear.

B. DISCUSSION OF RESULTS (μA744)

The pictures in Figure 11 are displayed in the same manner as those in Figure 5. These results from the first test show that as the circuit is subjected to a low-intensity portion of the beam a positive-going spike appears in the beam-pulse response. As the beam intensity increases the beam response changes polarity and its width increases; however, the positive spike is still present but with greater magnitude and a constant

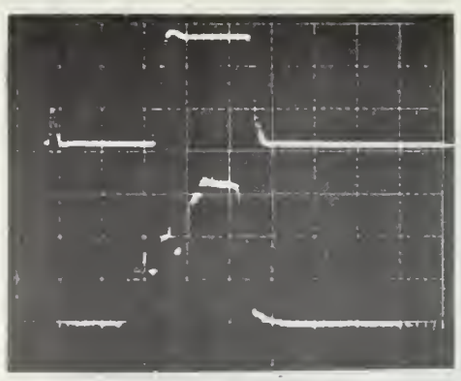

0.1 maximum
beam intensity

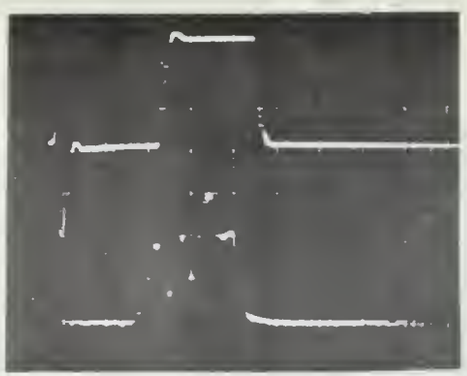

1/3 maximum
beam intensity

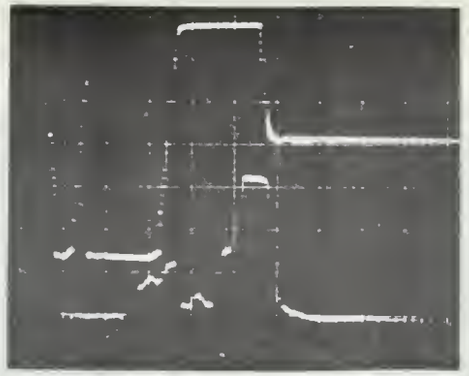

2/3 maximum
beam intensity

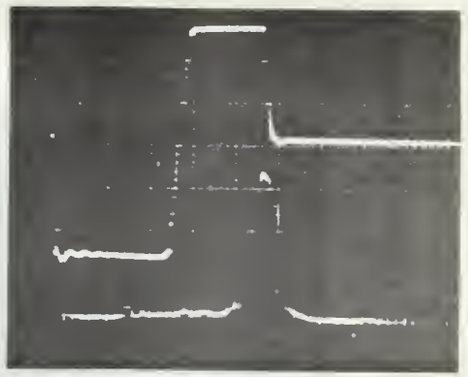

maximum
beam intensity

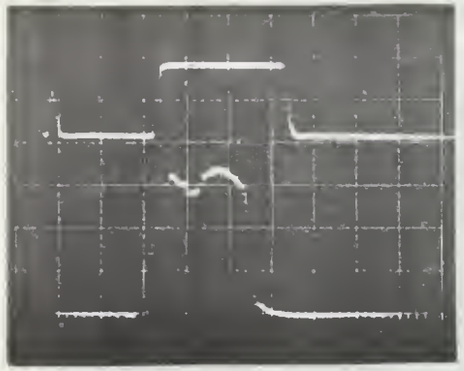

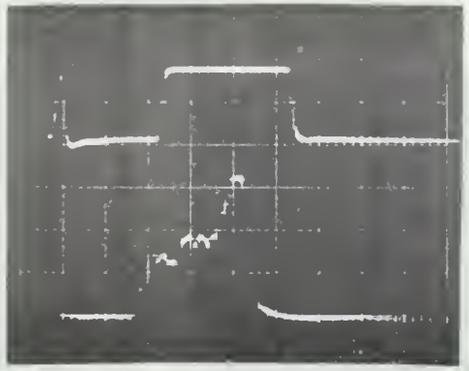

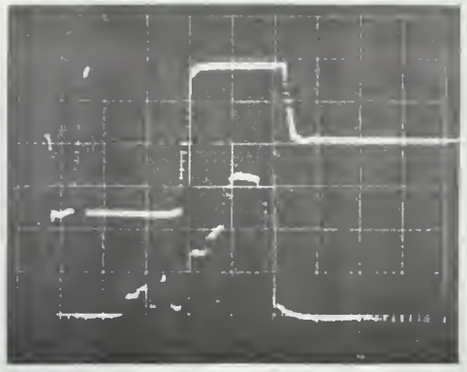

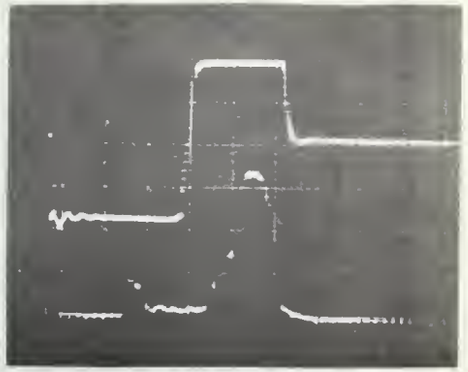

Upper Trace—Sweep: 5μsec/cm, Vert.: 0.1v/cm Lower Trace—Sweep: 0.2μsec/cm, Vert.: .05v/cm
Electronic Input Pulse—Amplitude: 10v, Width: 10μsec Top Row—V_S = ±15v Bottom Row—V_S = ±10v
(Traces are plotted in volts vs. time and the large scale squares measure 1cm on a side.)

Figure 11. μA744: First Test Responses

width. When the circuit is positioned so that it is receiving maximum beam intensity the spiked portion of the response disappears and very slight oscillations appear in its place. As the beam intensity is increased the beam-pulse response width widens to such an extent that it begins to affect the electronic-pulse response, causing it to lose its rise-portion overshoot and causing its recovery time to decrease slightly. This action did not affect the overall gain characteristics of the μA744. At no time in any μA744 response did strong oscillations appear.

In the second set of tests the purpose was to observe what happened to the amplifier's response to the beam and electronic pulses when supply voltages were decreased and the beam intensity remained essentially the same for each pulse. The data set groupings, the supply-voltage variations, and the display of results (Figures 12 and 13) were done in the same manner as were the second μA709 tests.

Figure 12 shows the responses for a simultaneous decrease in the two supply voltages (15, 7.5, 5.0, 2.5, 1.0 volts). As the supply voltages decreased so did the overall gain of the amplifier responses. The beam-pulse response recovery time increased to the point where it began to overlap the response from the electronic pulse. The recovery time of the electronic-pulse response also increased with decreased supply voltage despite the overlapping effect of the beam-pulse response. When the supply voltages reached a value of ±2.5 volts and lower, the lower responses were no longer present. In all cases, including a supply voltage of ±2.5 volts, the spiked portion of the beam-pulse response was present with a varying amplitude and an essentially constant width.

Figure 13 is the μA744 version of Figure 7. This set of pictures shows the effect of a reduction in one supply voltage, with the other held constant, on the beam and electronic-pulse responses. The top row

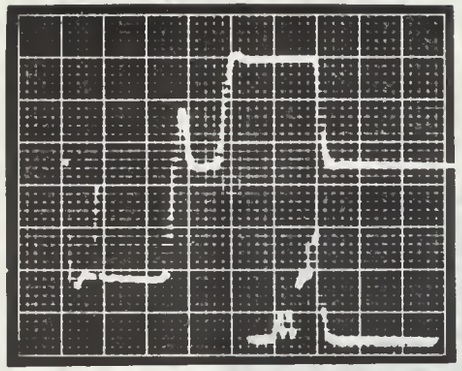

a. $V_s = \pm 15v$
5.7×10^3 rads

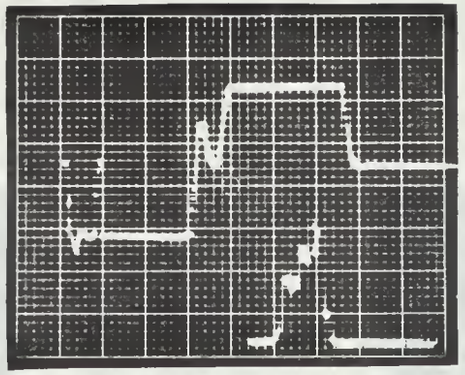

b. $V_s = \pm 10v$
7.4×10^3 rads

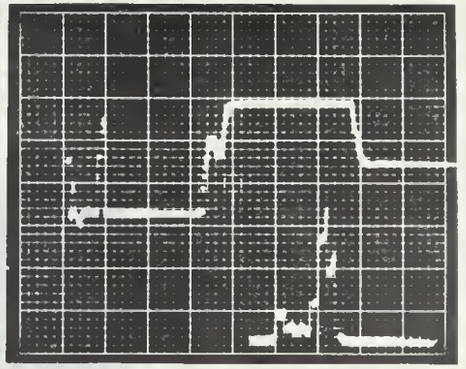

c. $V_s = \pm 7.5v$
5.7×10^3 rads

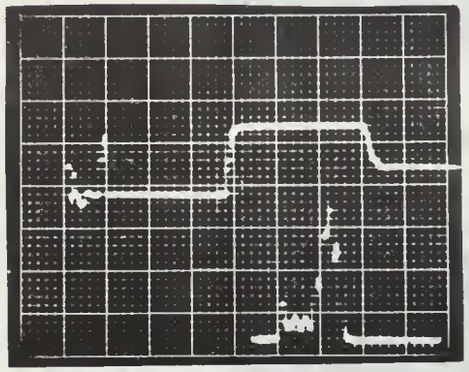

d. $V_s = \pm 5.0v$
6.3×10^3 rads

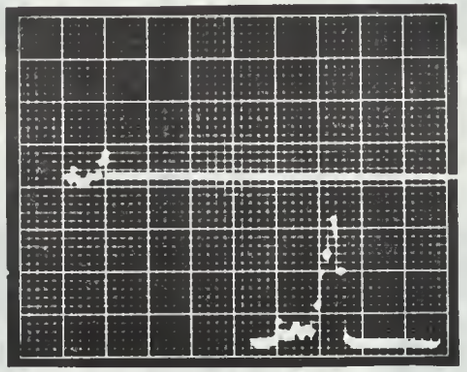

e. $V_s = \pm 2.5v$
6.3×10^3 rads

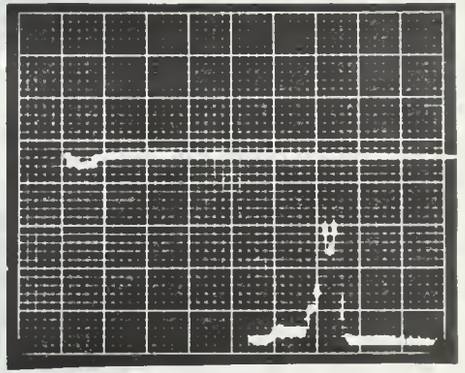

f. $V_s = \pm 1.0v$
6.3×10^3 rads

(Scaling, electronic input, trace plot, and large scale square parameters are the same as in Figure 6.)

Figure 12. μA744: Second Test Responses (Group 1)

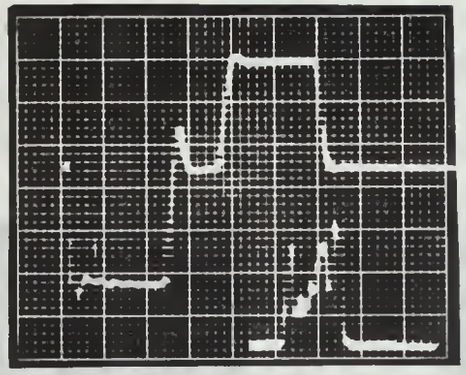

a. $V_s = \pm 15v$
8.6×10^3 rads

Group 2

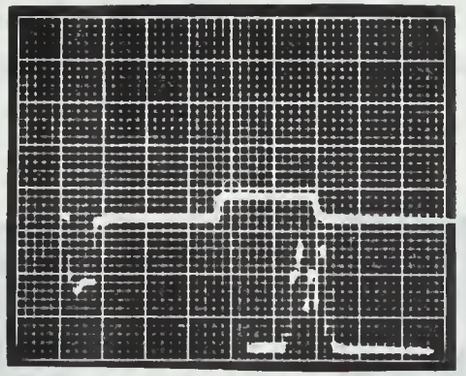

b. $V_s = +15, -1v$
6.8×10^3 rads

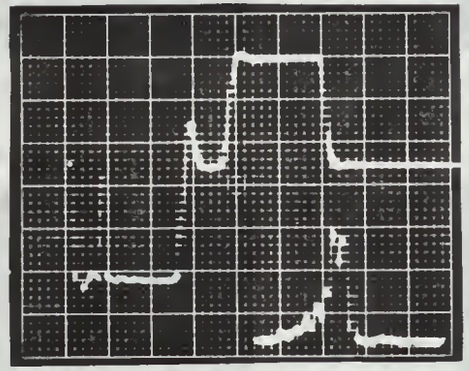

c. $V_s = \pm 15v$
6.3×10^3 rads

Group 3

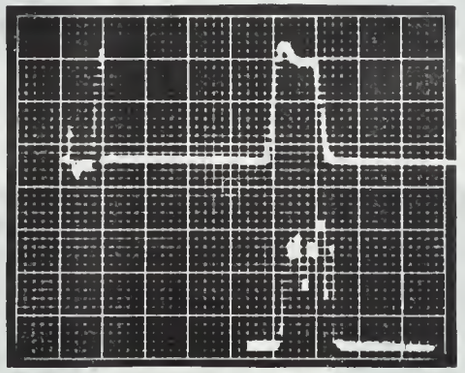

d. $V_s = +1v, -15v$
9.1×10^3 rads

(Scaling, electronic input pulse, trace plot, and large scale square parameters remain the same as in Figure 6.)

Figure 13. μA744: Second Test Responses (Groups 2 & 3)

shows that as the positive supply was kept at +15 volts and the negative supply reduced from -15 to -1 volt the magnitude of both responses was reduced. The recovery time of the beam-pulse response was reduced while the recovery time of the electronic-pulse response remained essentially constant. The spiked portion of the beam-pulse response disappeared when the negative supply was reduced -1.0 volt. The bottom row of pictures shows the positive supply reduced from +15 to +1 volt and the negative supply held constant at -15 volts. In this case the overall gain of the electronic-pulse response was unchanged while the gain of the beam-pulse response was reduced to zero. The recovery time of both responses was reduced significantly. In all reductions of the positive-supply voltage the spiked portion of the beam-pulse response remained present throughout as it did in the previous tests.

In order to see whether or not an accumulated dosage affected the spiked portion of the beam-pulse response the μA744 circuit was subjected to a dose of 4.6×10^7 rads and the supply voltages were reduced simultaneously from ±15v to ±1.0v. At this particular dosage accumulation the positive spike in the response disappeared altogether from the beam-pulse response for all values of reduced supply voltages. All responses in this test looked similar to those in Figure 12 except for the now absent spike.

VI. TESTS ON μA744 KIT PART KP-5

Table 2 gives the component and lead-bonding arrangement of the μA744 kit part KP-5. This particular kit part gave the opportunity to study the dielectrically-isolated versions of an NPN and PNP transistor.

The transistors of KP-5 were utilized in a common-emitter amplifier with an emitter-resistor test-circuit configuration to provide a response which gave a gain greater than 1 0. A self-biasing scheme was used because it was considered the best for stability. This type of amplifier is of the inverting variety The test circuits for the NPN and PNP transistors are shown in Figures 14 and 15 respectively. The numbers in the transistor circles denote the lead connections.

In order to provide impedance matching between the transistor output and the 63 feet of RG-58 triax cable connected to the Tektronix 556 oscilloscope, an emitter follower, located in the test box, was used (Figures 14 and 15).

In order to provide a suitable platform for the KP-5 test circuitry and sufficient radiation shielding, an aluminum test box (Figure 16) similar to that used in the test of the operational amplifiers was constructed.

Two tests were conducted on the KP-5 NPN transistor (Q_{11}). The first test was run with non-simultaneous perturbations of the device by the beam and electronic pulses. The second test was run with the beam pulse perturbing the circuit during the time it was amplifying the electronic pulse.

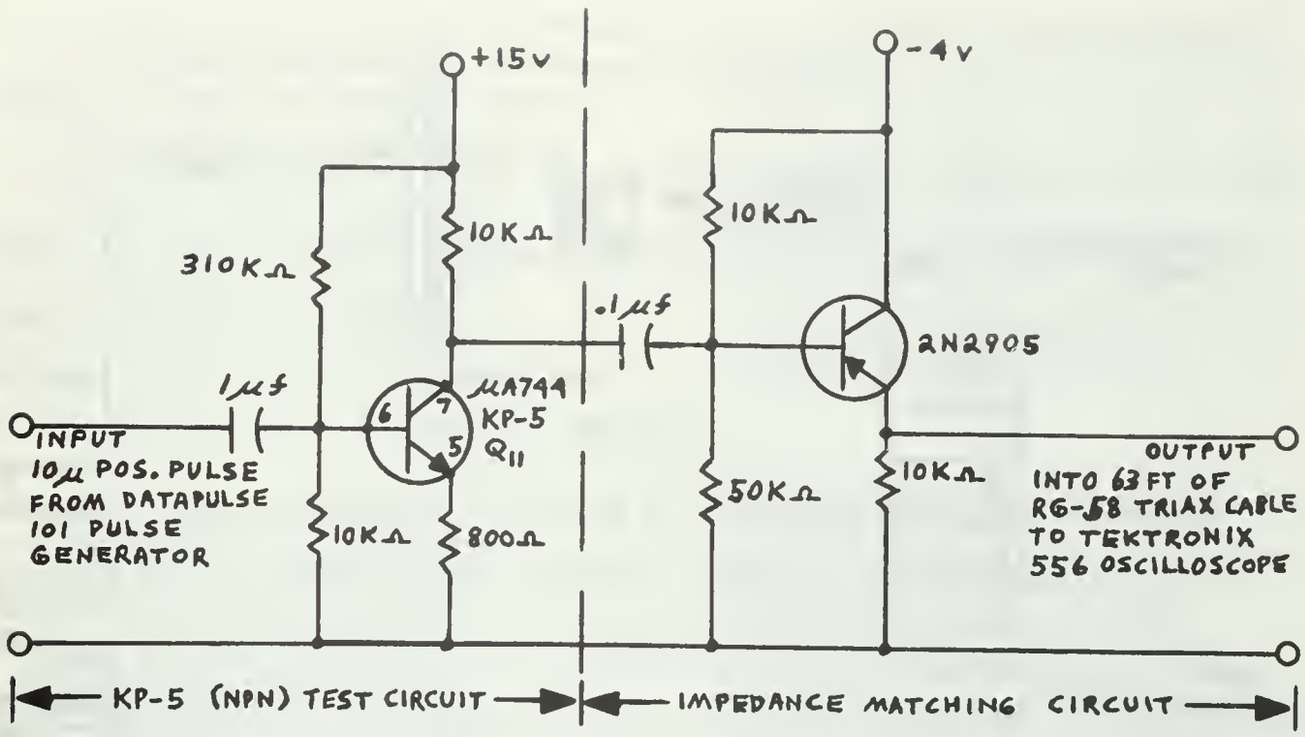

Figure 14. Schematic of μA744 KP-5(NPN) Test Circuit with Impedance-Matching Network

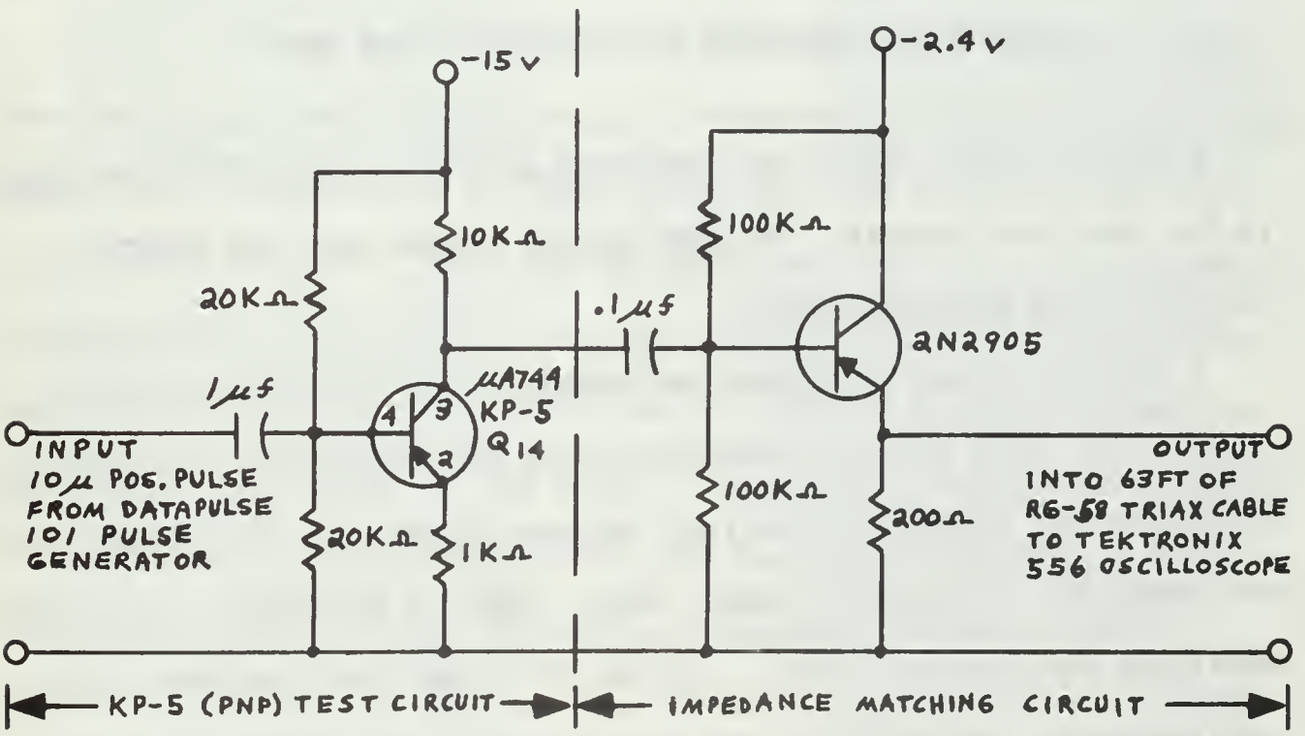

Figure 15. Schematic of μA744 KP-5(PNP) Test Circuit with Impedance-Matching Network

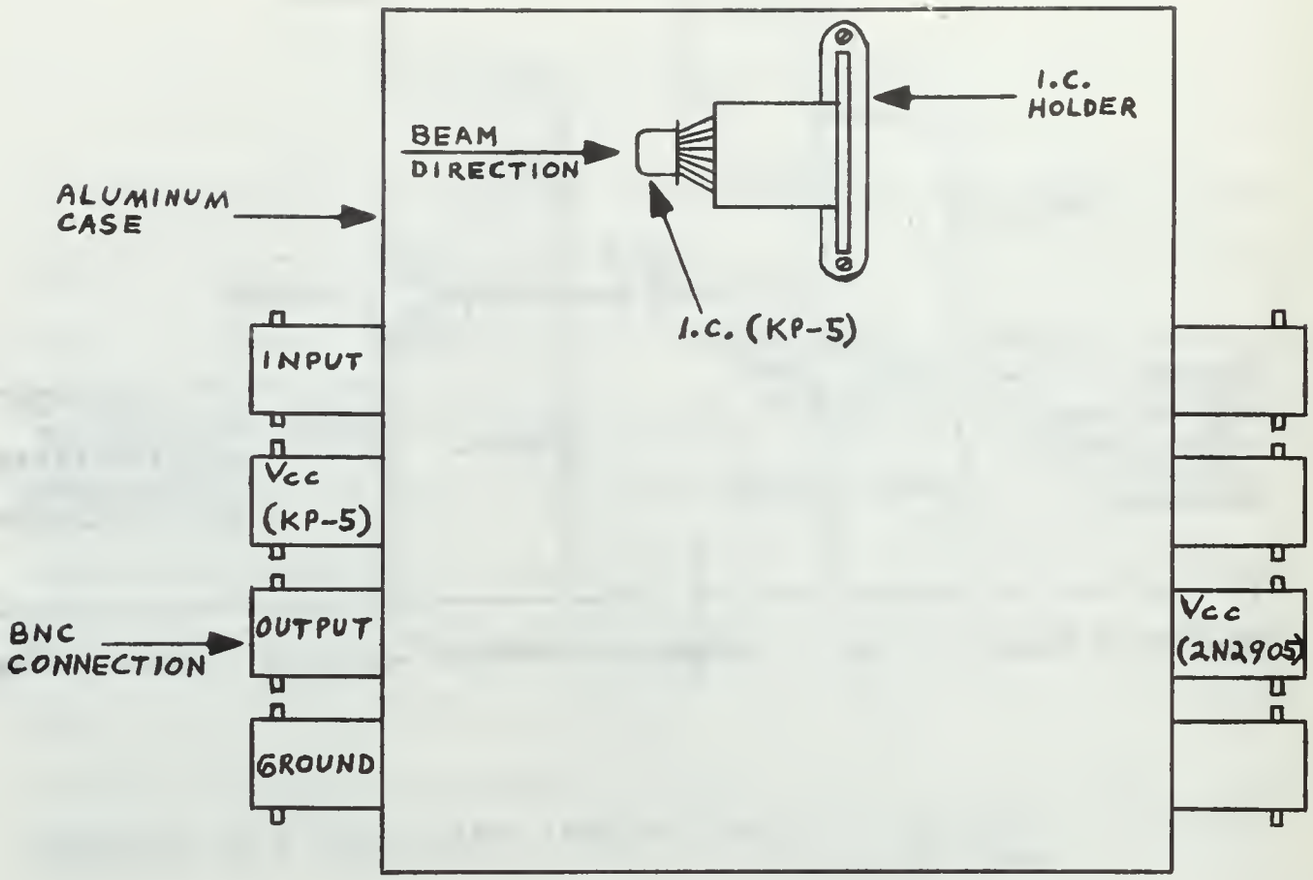

Figure 16. Top View of μA744 KP-5 Test Box

A set of similar tests was conducted on two discrete NPN transistors in the same test circuit. The two devices tested were the Motorola 2N2219 and the Raytheon 2N1613.

A series of four tests were performed on the KP-5 PNP transistor (Q_{14}). The first test was conducted using the lowest electronic-pulse level possible (0.45v) and varying the beam intensity. The second test was conducted in a similar manner except that the electronic-pulse input amplitude was doubled (0.90v). In the third test the electronic-input amplitude was 0.45 volts but the beam intensity was reduced to a very low value, so low in fact, that there was no appreciable measurement. The fourth test was conducted in the same manner as the first except that the horizontal-sweep scale was expanded to afford a better view of

the response. Also, the beam intensity was increased to a much higher value than in the previous tests.

Additional tests were run on two discrete PNP transistors in the same test circuit. The two devices tested were the Motorola 2N2905 and the Texas Instruments 2N1305.

A. DISCUSSION OF KIT PART TEST RESULTS

The primary reason for choosing an inverting amplifier as a test circuit was to reproduce an amplified, negative-going output response similar to that type of response obtained from the beam pulse in the μA744 amplifier. This was done so as to allow observation of the positive-going spike that might have occurred in the beam-pulse response during kit part testing. The following discussion will support this choice of test circuit.

Figure 17 shows the results of the NPN transistor simultaneous and non-simultaneous perturbation tests. These results show a negative-going beam-pulse response which is amplified in the same manner as the electronic-pulse response. When the two perturbations occur simultaneously the beam-pulse is all but lost in the response of the electronic pulse. There is no evidence in this NPN transistor of the positive-spiked response that was evident in the tests of the μA744. The discrete devices that were tested yielded essentially the same results as the KP-5 NPN transistor except that the beam-pulse response width was slightly greater in the discrete devices than it was in the KP-5 NPN transistor.

The results of the four sets of KP-5 PNP tests are contained in Figures 18, 19, 20, and 21. The first test results (Figure 18) show that for a low electronic input and low beam-pulse intensities the positive-going spike in the beam response appears as it did in the tests

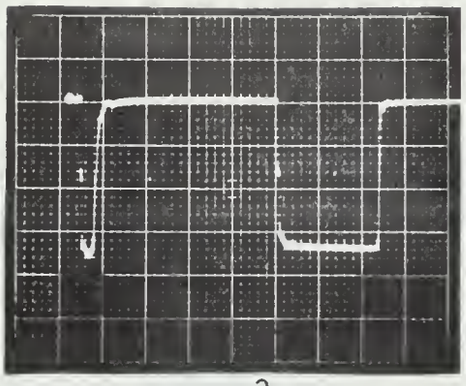

8.6×10^3 rads

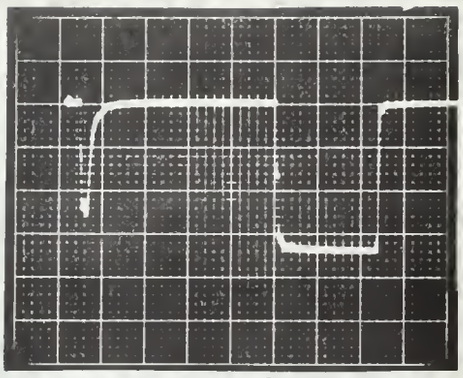

2.3×10^3 rads

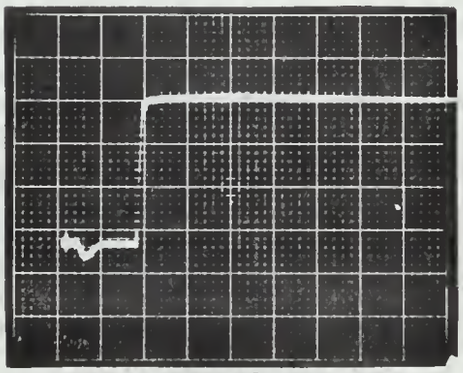

6.9×10^3 rads

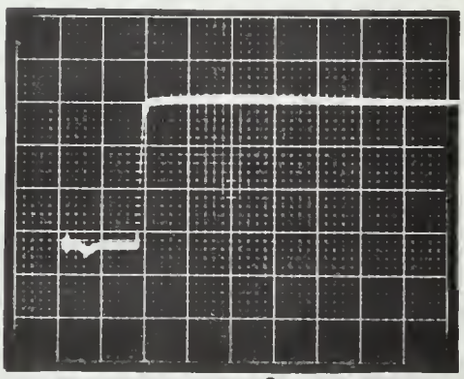

2.3×10^3 rads

Sweep: 5μsec/cm, Vertical: 0.2 v/cm, Input pulse—amplitude 0.45v, width: 10μsec
(Trace plots are volts vs. time and large-scale squares measure 1 cm on a side.)

Figure 17. KP-5 Transistor Test Results

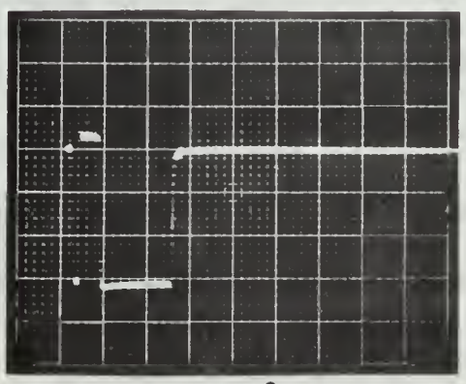

1.0×10^3 rads

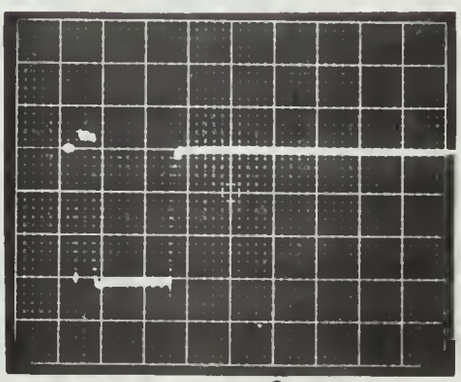

2.6×10^2 rads

Sweep: 5μsec/cm, Vertical: 0.2v/cm, Input pulse—amplitude: 0.45v, Width: 10μsec
(Trace plot and large-scale square parameters are as in Figure 17.)

Figure 18. KP-5 PNP Test 1 Results

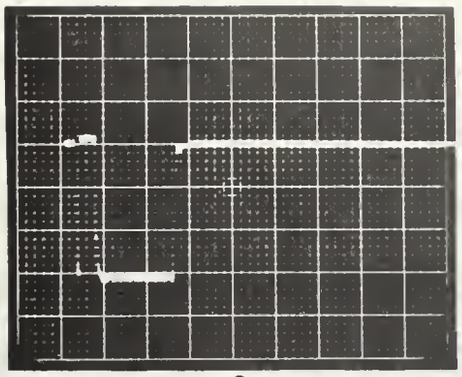

$1.1x10^3$ rads

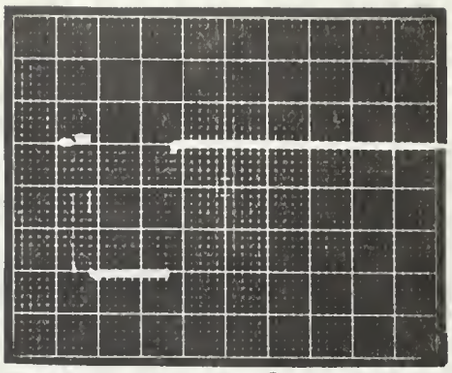

$4.0x10^2$ rads

Sweep: 5μsec/cm, Vertical: 0.5v/cm, Input pulse—amplitude: 0.90v, width: 10μsec
(Trace plot and large-scale square parameters are as in Figure 17.)

Figure 19. KP-5 PNP Test 2 Results

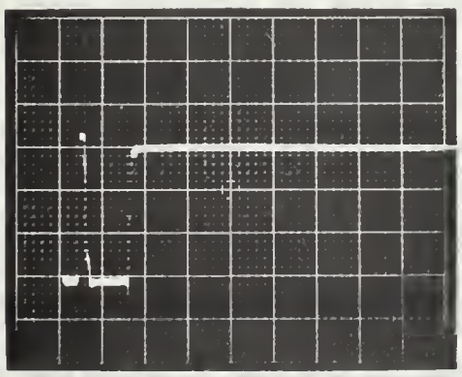

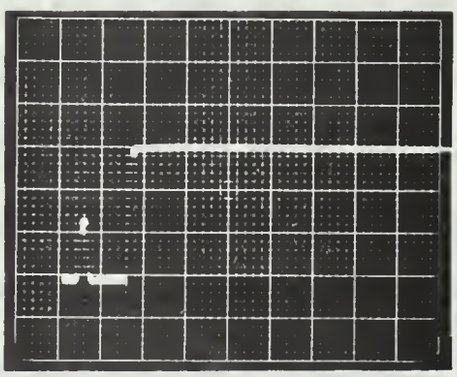

(Sweep, vertical, input pulse, trace plot, and scale square parameters are the same as in Figure 18.)

Figure 20. KP-5 PNP Test 3 Results

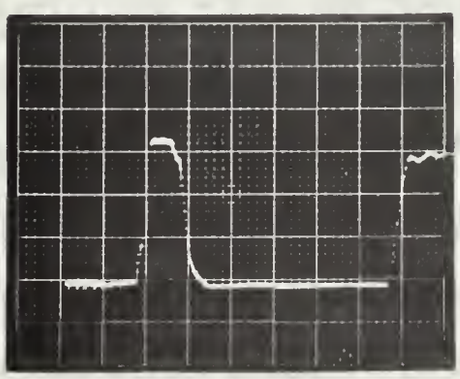

$3.4x10^2$ rads

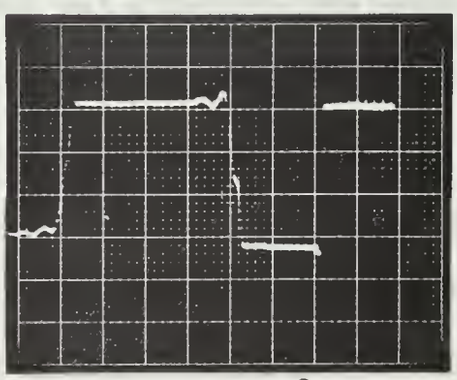

$6.9x10^3$ rads

Sweep: 1μsec/cm — all other parameters are as in Figure 18

Figure 21. KP-5 PNP Test 4 Results

on the μA744 amplifier. In this test the amplitude of the spiked portion is flat because the transistor has been driven into saturation at this point. Even in the second test (Figure 19) with the input amplitude doubled, the positive-going spike is still in the response and again the amplifier is driven into saturation. In the third test the beam intensity was reduced so much that it could not be read on the electrometer; however the spike in the beam response now resembles that found in the μA744 amplifier (Figure 20). In this test the reduction in beam intensity reduces very slightly the spike width and a larger reduction causes the amplitude of the spike to drop with no furthur reduction in spike width. The fourth test results (Figure 21) show an expanded view of the spike in the response. As the intensity of the beam is increased from a low value the amplitude is driven further into saturation and the spike width increases by a factor of two

The absence of the positive-going spike in the beam-pulse response of the KP-5 NPN transistor and its presence in the PNP transistor's response is of importance in explaining its presence in the μA744 amplifier responses. Since the PNP transistor tested is Q_{14} in Figure 2 this means that the presence of this type of transistor in the output of the μA744 amplifier accounts for the generation and passage of the positive-going spiked response directly into the output response of the μA744 amplifier.

The tests performed on the two discrete PNP transistors yielded responses similar to those in the KP-5 PNP transistor tests. The major difference was that the spike width was twice as large in the discrete transistors as in the KP-5 PNP transistor. This leads to the conclusion that the transistor in the μA744 has a faster recovery time than its discrete counterpart.

VII. COMPARISON OF RESULTS: μA709 VS. μA744

The results of testing the μA709 and μA744 amplifiers indicate that there are some differences in their responses in a radiation environment of the type used in this study.

One difference is the presence of very strong oscillations in the μA709 beam-pulse response and the absence of the oscillation in the μA744. Although these oscillations did not appear in the Fairchild flash X-ray testing conducted at the Fairchild Semiconductor laboratories, it is significant to note that in the tests performed by the author both the μA709 and μA744 amplifiers were tested in the same test circuit and under identical conditions. However, strong oscillations appeared only in the μA709 and only in the μA709's beam-pulse response, not the electronic-pulse response. Although it was felt that the oscillations were caused by too low decoupling capacitance in the test circuitry the significant response difference was still present even when the decoupling capacitance was increased from 0.01 to 0.22-microfarads. Thus it appears that the oscillations in the μA709 depend a great deal on the radiation environment.

The μA744 differs from the μA709 in that its beam-pulse response contains a positive-going spike within the total response (see Figure 12). This was not identifiable in the μA709 tests because of the strong oscillations. Further, in his transient tests on the μA709, Lesemann found no such spike in his responses. This spike appears to have been generated and passed to the output by the PNP output transistor Q_{14}.

The tests in this study revealed that the μA709 amplifier operates best in this type of radiation environment after some accumulated dosage,

the optimum being somewhere around 1.3×10^8 rads and a beam-pulse intensity of less than 2.9×10^2 rads

The spike in the beam-pulse response of the μA744 disappears completely after having accumulated a dosage of approximately 4.6×10^7 rads. The spike does not return as the dosage is increased.

VIII. CONCLUSIONS AND RECOMMENDATIONS

In an ideal situation a perfectly radiation-hardened device would not yield an observable electronic response when subjected to a radiation environment. This ideal hardening scheme is obviously not present in the μA744, and when viewed from this ideal aspect the μA744 is not superior to the μA709. In considering only radiation responses the μA744 is superior to the μA709 in that it produces a much better pulse shape in its radiation response. The exception to this statement was the presence of the spike in the beam-pulse response. It was determined that this spike was a product of the μA744's output transistor Q_{14}, one of the two such PNP transistors in the whole amplifier.

The dielectrically-isolated NPN and PNP transistors of the μA744 produced response-pulse widths much narrower than those from the corresponding discrete transistors. It was not determined what responses were produced by the NPN transistors of the μA709 because of the inability to test these devices.

Since it was shown that both the μA709 and the μA744 perform better after having accumulated certain amounts of radiation dosage it is recommended that the causes and mechanisms of this effect be investigated in greater detail. It is also recommended that the following further studies be made. A detailed investigation should be conducted by monitoring photocurrent flows between the three stages of the amplifiers to determine what effect dielectric isolation and photocurrent-compensation diodes have on the μA744 as compared to the μA709. Tests of this kind would necessitate the manufacture of kit parts containing just the separate amplifier stages. Also, the μA709 kit part transistors should

be investigated. This investigation should consider comparison of the kit part transistors with the off-the-shelf varieties, a detailed look at what effect the substrate has on radiation response, and a comparison of the substrate connected μA709 kit part elements with the dielectrically-isolated elements of the μA744.

APPENDIX A
CALCULATION OF DOSE AND DOSE RATE

A vibrating-reed electrometer was used to measure the voltage across a 1-microfarad capacitor charged by the electrons collected in a Faraday cup. The number of electrons hitting the Faraday cup can be determined from the voltage on the capacitor as follows:

$$C = Q/V$$

$$V = (10^6)(Q)$$

Q = charge collected by Faraday cup = $(1.6\times10^{-19})N$

N = number of electrons hitting the cup

Thus $$V = (1.6\times10^{-19})(10^6)(N) = (1.6\times10^{-13})N$$

$$N = \frac{V}{1.6}(10^{13})$$

A typical single pulse with full beam intensity yields approximately a 20mv reading on the electrometer.

Thus, $N = 1.25\times10^{11}$ electrons/pulse

The effects of an electron beam passing through a thin piece of semiconductor material are twofold. First, γ-rays are produced by the electron beam and, secondly, low-energy electrons, called δ-rays, are produced by ionizing collisions. These δ-rays are the cause of semiconductor photocurrents. In considering the energy deposited in the semiconductor material the γ-rays are ignored because their mean free path is much greater than the thickness of the semiconductor material or the operational amplifier. What is considered is the energy loss by the incident electrons when causing ionization and thus the creation of the δ-rays. At energies higher than about 50Mev the energy loss (per unit

path) remains essentially constant. The NPS LINAC runs in excess of 50Mev and in this region the energy loss is independent of incident energy. The value used is

$$\alpha = 1/\rho \frac{dE}{dx} = 1.90 \left(\frac{\text{Mev cm}^2}{\text{gm}}\right) \text{ for silicon.}$$

Where ρ = density of semiconductor material

and $\frac{dE}{dx}$ = energy loss (Mev/cm).

If $\dot{\phi}$ denotes electron flux (elect./cm^{2}sec)

then $\phi = \int \dot{\phi}\, dt$ = fluence = elect/cm^2.

The dose rate and dose can be calculated as follows:

Dose Rate = $\dot{D} = \alpha\dot{\phi}$ = Mev/gm sec (1Mev = $1.6\text{x}10^{-6}$ ergs)

$\dot{D} = (1.6\text{x}10^{-6})(\alpha\dot{\phi})$ = ergs/gm sec (1 rad = 100 ergs/gm)

$\dot{D} = (1.6\text{x}10^{-8})(\alpha\dot{\phi})$ = rads/sec .

Dose = $D = \int \dot{D}\, dt$ = rads

$D = (1.6\text{x}10^{-8})(\alpha\phi)$.

Consider a single electron-beam pulse as an example. Let the area of the beam be 1/3 cm^2.

Thus $N = V/1.6\ (10^{13}) = (.625\text{x}10^{13})(V)$ = No. electrons/pulse.

$\phi = (1.88\text{x}10^{13})(V)$ = electrons/cm^2

$\alpha\phi = (3.57\text{x}10^{13})(V)$

Therefore $D = (1.6\text{x}10^{-8})(3.57\text{x}10^{13})(V) = (5.7\text{x}10^{5})(V)$

Since the beam pulse time was $1\text{x}10^{-6}$ sec and a typical electrometer reading at full beam was 20mv we have:

$\dot{D} = (5.71 \times 10^{5})(20 \times 10^{-3})(10^{6}) = 1.1 \times 10^{10}$ rads/sec, and

$D = 1.1 \times 10^{4}$ rads .

Various methods of dosimetry have been used to verify these calculations. It is estimated that the measurements are accurate to within a factor of two.

BIBLIOGRAPHY

1. Giles, J. N., Fairchild Semiconductor Linear Integrated Circuits Applications Handbook, p. 57-72, Fairchild Semiconductor, 1967.

2. Widlar, R. J., "A Unique Circuit Design for a High Performance Operational Amplifier Especially Suited to Monolithic Construction," Proceedings of the National Electronics Conference, October 1965.

3. MacDougall, J. S., Oberlin, D. W., and Stafford, K. R., "The Design of Radiation Hardened Integrated Circuit Operational Amplifiers," GOMAC Digest of Papers, p. 326-329, October 1968.

4. Fairchild Semiconductor Application Brief-122, A Monolithic Radiation-Resistant Operational Amplifier, June 1969.

5. Fairchild Linear Integrated Circuits Preliminary Data Sheet, μA744 Radiation-Resistant Operational Amplifier, p. 1, August 1969.

6. Lesemann, D. F., Comparisons Between Radiation Hardened and Standard Integrated Circuit Amplifiers in an Electron Beam, M. S. Thesis, Naval Postgraduate School, Monterey, April 1969.

7. Fairchild Linear Integrated Circuits Data Sheet SL-64/A, μA709 High Performance Operational Amplifier, p. 4, April 1966.

INITIAL DISTRIBUTION LIST

		No. Copies
1.	Defense Documentation Center Cameron Station Alexandria, Virginia 22314	20
2.	Library, Code 0212 Naval Postgraduate School Monterey, California 93940	2
3.	Commandant of the Marine Corps (Code A03C) Headquarters, U. S. Marine Corps Washington, D. C. 20380	1
4.	James Carson Breckinridge Library Marine Corps Development and Educational Command Quantico, Virginia 22134	1
5.	Captain Patric S. Enright, USMC P.O. Box 113 New Market, Virginia 22844	1
6.	Professor J. N. Dyer Department of Physics Naval Postgraduate School Monterey, California 93940	4
7.	Professor Shu-gar Chan Department of Electrical Engineering Naval Postgraduate School Monterey, California 93940	1
8.	Linear Accelerator Facility Naval Postgraduate School Monterey, California 93940	3
9.	Fairchild Semiconductor R and D Lab Linear Integrated Circuits Section 4001 Miranda Blvd. Palo Alto, California 94304	5

Security Classification

DOCUMENT CONTROL DATA - R & D

(Security classification of title, body of abstract and indexing annotation must be entered when the overall report is classified)

1. ORIGINATING ACTIVITY *(Corporate author)*

Naval Postgraduate School
Monterey, California 93940

2a. REPORT SECURITY CLASSIFICATION

Unclassified

2b. GROUP

3. REPORT TITLE

A Study of Transient Radiation Effects on the Response of Standard and Radiation-Hardened Integrated-Circuit Operational Amplifiers in an Electron Beam

4. DESCRIPTIVE NOTES *(Type of report and inclusive dates)*

Master's Thesis, December 1969

5. AUTHOR(S) *(First name, middle initial, last name)*

Patric Stam Enright

6. REPORT DATE	7a. TOTAL NO. OF PAGES	7b. NO. OF REFS
December 1969	51	7

8a. CONTRACT OR GRANT NO.	9a. ORIGINATOR'S REPORT NUMBER(S)
b. PROJECT NO.	
c.	9b. OTHER REPORT NO(S) *(Any other numbers that may be assigned this report)*
d.	

10. DISTRIBUTION STATEMENT

This document has been approved for public release and sale; its distribution is unlimited.

11. SUPPLEMENTARY NOTES	12. SPONSORING MILITARY ACTIVITY
	Naval Postgraduate School Monterey, California 93940

13. ABSTRACT

This study investigates the effects of 1-μsec pulses of 80 - 90 Mev electrons on the standard μA709 operational amplifier and its radiation-hardened version, the μA744. The transient responses from the electron beam and from electronic pulses were investigated and compared for each amplifier. Also investigated were the responses of dielectrically isolated NPN and PNP transistors contained in the μA744, which were further compared with responses obtained from discrete NPN and PNP transistors.

The overall transient radiation responses of the μA709 and μA744 amplifiers, with several exceptions, were not very different. The same can be said for a comparison of the responses from the μA744 and discrete NPN and PNP transistors. Based on this study the μA744 is not superior to the μA709 by virtue of its radiation hardening. It should be noted, however, that the μA709 is driven into oscillation by the electron beam while the μA744 is not.

DD FORM 1 NOV 65 1473 (PAGE 1)

S/N 0101-807-6811

Security Classification

A-31408

14 KEY WORDS	LINK A		LINK B		LINK C	
	ROLE	WT	ROLE	WT	ROLE	WT
Operational Amplifier						
Linear Accelerator						
Electron Beam						

DD FORM 1 NOV 65 1473 (BACK)

S/N 0101-807-6821